Automatic Identification of Inflection Points in Pressure and Regional EIT curves

Ravi Bhanabhai*, Inez Frerichs†, Sven Pulletz† and Andy Adler *,
*Systems and Computer Engineering
Carleton University, Ottawa, Canada
Email: {rbhanabh, aadler}@sce.carleton.ca
† Department of Anesthesiology and Intensive Care Medicine
University Medical Center Schleswig-Holstein, Campus Kiel, Kiel, Germany
Email: {frerichs, pulletz}@anaesthesie.uni-kiel.de

***Abstract*—Ventilator Induced Lung Injury (VILI) is a serious condition caused by sub-optimal settings of mechanical ventilation in Acute Lung Injury (ALI) patients. The main contributors to VILI are 1) cyclic opening and closing of collapsed lung tissue which occur at low pressure and 2) overdistension of lung tissue which occur at high pressures. Reducing these within mechanically ventilated patients can lead to an increase in likelihood of survival. The key clinical measure to reduce VILI is selecting an appropriate Positive-End Expiratory Pressure (PEEP) to make a balance between keeping lung units open while not overdistending them. Electrical Impedance Tomography (EIT) provides regional lung air volume information which promises to help improve clinical selection of PEEP. The goal of this paper is to compare two automated methods (three-piece linear and sigmoid models) and one manual method (visual heuristics) in the analyse of EIT data to locate regional inflection points (IP). These IP can be used to distinguish between collapsed and overdistended regions, thus assisting in the location of a best suited PEEP. These algorithms were implemented, tested, and compared to previously suggested approaches, using a clinical database of ALI and healthy lung patients. Results varied depending on which IP was being compared. Comparing the visual heuristic method with the linear spline method differences ranged from -1.507 mbar to 0.0240 mbar. The results are promising and continued work on the linear method in IP selection is suggested.**

I. Introduction

The lung is an essential organ within the respiratory system with its main function being the transport of oxygen into the bloodstream while also moving carbon dioxide out of the bloodstream. Respiratory failure is a medical condition where the patient is unable to adequately control the transaction of blood-gases. It can come on abruptly as seen with acute respiratory failure or slowly as seen with chronic respiratory failure. Typically, respiratory failure initially affects the transfer of oxygen to the blood or the removal of carbon dioxide from the blood [1]. Oxygenation Failure usually is a sign of ALI and is discussed in this paper. For further information on Ventilatory Failure (failure to remove carbon dioxide) refer to Chapter 20 from [1].

A. Acute Lung Injury

Acute Lung Injury is the umbrella term used to describe hypoxemic respiratory failure. ALI covers Acute Respiratory Distress Syndrome but also other milder degrees of lung injury [1]. Normal alveoli have an inner layer of surfactant which helps to keep the lung tissue open during expiration, in diseased lungs this surfactant is lacking making the alveoli unstable and prone to collapse. When diseased lung tissue are repeatedly open and closed shear stresses are generated, which can produce ruptures causing damage [2]. To treat ALI mechanical ventilation systems are used to alleviate the work of breathing. Either pressure controlled or volume controlled systems are used. A crucial support strategy is to set and maintain the Positive-End Expiratory Pressure (PEEP). PEEP is a pressure support system used during exhalation to help maintain open lung regions leading to better oxygenation and reduction of cyclic opening and closing of lung tissue. Normal selection of PEEP is done by an iterative procedure where PEEP is adjusted till an appropriate oxygenation is reached. Each step in PEEP usually takes around 15-20 minutes in order for the oxygenation to reach steady state [2]. Because of the heterogeneous nature of lung tissue in ALI/ARDS patients not all of the alveoli are collapsed at the same time thus while some tissue are opening others can be overdistending lending to Ventilator Induced Lung Injury (VILI) [2], [3]. Injuries in ventilated ARDS patients can lead to further alveolar ruptures causing complications such as pneumothorax. This case tends to happen when excess airway pressures is used and is commonly referred to barotrauma or alveolar overdistension. In addition to overdistension, injury from ventilation systems can be caused by cyclic opening and closing of lung units. This cyclic action releases cytokines, a protein transmitter released during inflammatory response. This can be remedied by keeping lung units open via PEEP thus reducing the opening and closing behavior but insurances must be made to avoid overdistension which can lead to barotrauma [4].

To pick a well suited PEEP, pressure-volume (pv) curves have been used as a means to guide ventilation settings [3]. From the pv curves inflection points (IP) are located for the use in guided ventilation.

B. Inflection Points

In this context inflection points are the locations along a pressure-volume curve, or with the use of EIT pressure-

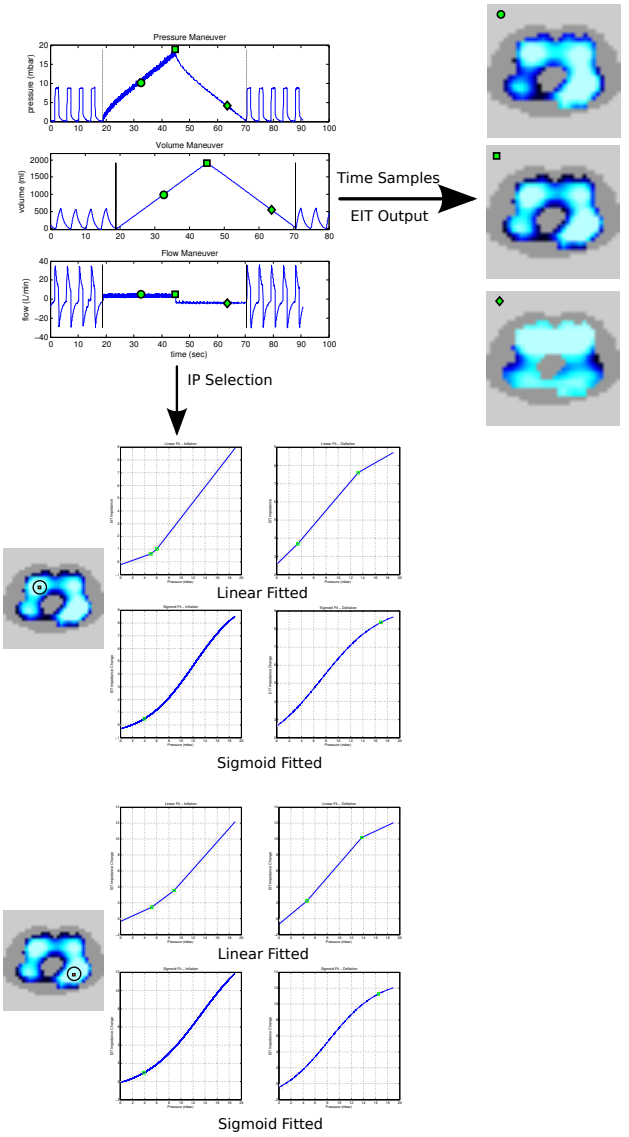

Fig. 1: Example of pressure, volume, and flow maneuver used. The cyclic behavior before and after the black lines in the recruitment portion of the figure are of patient ventilation. Example EIT images are shown to the right of the recruitment portion with indication of time index shown by the corresponding shapes in each EIT reconstruction. The bottom portion of the figure shows both the Linear and Sigmoid fitted data with the corresponding data originating from location shown to the right of the fitted graphs.

impedance curves where the slope dramatically changes usually from a low compliance region to a high compliance region or a high compliance region to a low one. There exists multiple ways of locating IP [5] with this paper exploring the sigmoid method, visual heuristics, and the 3-piece linear spline method. The use of inflection points in clinical settings are well known and are currently used in global pv curves to set the base-pressure (PEEP) in Acute Lung Injury (ALI) patients [6], [5]. The work on inflection points is important as it is one of the common methods for optimizing PEEP in mechanical ventilation [7], [8]. The goal of this paper was to evaluate the accuracy and repeatability of locating inflection points within impedance based images.

II. Methodology

Electrical Impedance Tomography is an imaging modality that is non-invasive, non-ionizing and relatively inexpensive (thousands of dollars) [9]. It produces a 2D conductivity image of a medium. With respect to imaging lung aeration the volumetric accuracy of an EIT system is within 10% of spirometric measurements [10]. This is of particular significance since the air distribution within pathological lungs is heterogeneous [11]. Large impedance differences between inflated ($12.5\Omega m$) and deflated ($25.0\Omega m$) lung tissue makes the use of EIT as a regional bedside tool quite appealing [10], [12]. An example image from an EIT system is shown in Fig. 1 on the top right hand side, the figure shows three separate moments in time and their respective EIT output. Similar to how global pressure-volume curves can be used for guided ventilation the use of regional impedance information can be used to create pressure-impedance curves which in turn can be used for PEEP selection. The benefit here is the use of regional information to select PEEP values.

A. Data

The data used within this study was conducted by [13]. It consisted of a low-flow pressure based recruitment maneuver with synchronized EIT. Human trials were performed from the medical university center at Schleswig Holstein campus in Kiel.

1) Patient: The experiment received local ethics approval for 26 patients and were taken from the surgical intensive care unit and the operations theaters. Written consent was taken from each patient or a legal representative. All patients were sedated, paralyzed, and artificially ventilated using a pressure controlled ventilation mode while in the supine position. The 8 healthy lung patients were 41 ± 14 years of age, 177 ± 8cm in height, 76 ± 8kg in weight, while the 18 ALI patients were 58 ± 14 years of age, 177 ± 9cm in height, 80 ± 11kg in weight (mean $\pm$ SD). All patients fulfilled the American-European consensus criteria for ALI (rapid onset, $\frac{P_aO_2}{FIO_2} \leq 400$ mbar, bilateral infiltrates, and no clinical sign of left atrial hypertension).

2) Pressure Maneuver: The pressure maneuver used was performed using an Evita XL (Draeger, Luebeck, Germany) mechanical ventilator. The maneuver started at zero Positive-End Expiratory Pressure (0 PEEP) and stopped when a tidal volume of 2L was met or a max airway pressure of 35 mbar. Fig. 1 illustrates a sample of the pressure, volume, and volume flow in which the data samples before and after the vertical black lines are of the patient being ventilated, while the data in-between is of the recruitment maneuver. The mechanical ventilator sampled the input data at a rate of 126Hz and was synchronized to an EIT data acquisition system via USB, with a sample rate of 25Hz. The EIT data was gathered using a GOE-MF II EIT system (CareFusion, Hoechberg, Germany) with 16 self-adhesive electrodes (Blue sensor L-00-S, Ambu, Ballerup, Denmark). The electrodes were positioned

approximately along the 5^{th} intercostal plane and were evenly distributed around the circumference of the patient. 50kHz and 5 mA_{rms} electrical current was applied through an adjacent pair configuration with the remaining electrodes being used to measure the voltage after the current injection.

B. Data Analysis

To locate inflection points multiple methods exist with this paper testing three methods. The first method discussed is the visual heuristic method. Many clinics already use this method to locate inflection points and is done manually by a physician. The second and more classic automated method is the sigmoid method. This is an automated method which fits the pressure-impedance data to a sigmoid function [6], [14]. The third method tested is the three-piece linear spline method [14]. This is another automated method which fits the pressure-impedance data to three linear segments.

1) Visual Heuristic: In the clinical setting inflection points are located by the clinician using their expert knowledge from global pressure-volume curves. Variability between visual based inflection points exist leading to more automated methods [5]. [15] also tested the visual heuristic method on a linear segmental regression method and found a correlation of 0.54 and 0.84 for the lower and upper inflection points respectively. For this paper four pixels from each patient were tested and five volunteers were ask to fit three linear segments to the data. All the volunteers expect one had an engineering background with the other having an English background. The location of the inflection points were taken as the points where the two lateral line segments intersected the median line. Each participant worked with both the inflation and deflation arms of the recruitment maneuver thus fitting a total of eight pressure-impedance curves per patient.

2) Sigmoid Method: [6] introduced the use of the sigmoid method as an automated method to find inflection points and has been used by many other researchers since [14], [16], [17], [5]. With the use of the sigmoid method in global pressure-volume curves clinicians were able to locate both upper and lower inflection points to help reduce cases of cyclic opening and closing and overdistension. An example of a sigmoid fitted pressure-impedance curve can be seen in Fig. 1.

The sigmoid method fits the data to (1) where V is the inflation or absolute volume, P is the airway or transpulmonary pressure, a is the volume corresponding the lower asymptote which is used to approximate the residual volume when absolute volume is used, b is the vital capacity or total volume change between the two asymptotes, c is the pressure at the highest compliance and is also the true inflection point, and d is proportional to the pressure range where most of the volume changes takes place, or in other words it's the pressure difference between the actual inflection and the zone of high compliance. The inflection points are located using (2) which are also the locations where the tangents from the two asymptotes intersect with the tangent at the best compliance ($P = c$). Constraints on the final parameters were also set in order to achieve logical solutions. For parameters b, c, d a lower bound of 0 was set while parameters c, d had an upper bound of the maximum pressure. All other constraints were set to $-\infty$ and ∞. The initial search parameters used were $a = min(\text{of impedance})$, $b = max(\text{of impedance}) - min(\text{of impedance})$, $c = median(\text{of pressure})$, $d = 0.5$.

$$V = a + \left[\frac{b}{1 + e^{-(P-c)/d}}\right] \tag{1}$$

$$P_{u,l} = c \pm 2d \tag{2}$$

3) Linear Spline Method: The three piece linear spline fits pressure-impedance curves with three linear segments with optimal break point locations. (3) shows the mathematical definition where a indicates the respective slopes, b the respective y-intercept, P is the pressure, V/I is the volume/impedance, LI is the lower inflection point, and UI is the upper inflection point. The MATLAB implementation was designed and coded by John D'Errico [18]. In this paper to ensure three distinct line segments were placed the length of each segment was set to a minimum of 1 mbar. The inflection points were taken as the locations where each line segments meets its adjacent which is also the location of the break points. An example of a three-piece fitting can be seen in Fig. 1. The linear spline method is preferred over the sigmoid method because of its resemblance to manual curve analysis [16]. Despite the relative novelty of this method it has great intuitive appeal as it picks out the location of the high compliance regions rather easily which has shown to resemble normal lung function [19].

$$V/I = \begin{cases} a_1 P + b_1 & 0 \leq P \leq \text{LI} \\ a_2 P + b_2 & \text{LI} \leq P \leq \text{UI} \\ a_3 P + b_3 & \text{UI} \leq P \end{cases} \tag{3}$$

III. Results

This section illustrates the results between the comparison of the inflection points found between the: linear and sigmoid methods, the linear and visual heuristic methods, and the sigmoid and visual heuristic methods.

A. Linear Spline vs. Sigmoid

Comparing the linear and sigmoid method was done by seeing how often each respective methodology was able to locate an IP. The linear method was able to find inflection points 99.95% of the time while the sigmoid method was able to an inflection point 57.13% of the time. The sigmoid method had an interesting trend in that it rarely would find both inflection points. It would locate either the lower or upper but hardly ever both. Fig. 2 illustrates the distribution of how frequent an inflection point was not found.

B. Linear Spline vs. Visual Heuristic

When selecting the human based inflection points each participant has only one chance to place the inflection point thus medians over the participants were taken to help reduce the effects of placement error. Each participant fitted the same pressure-impedance curves providing continuity between participants.

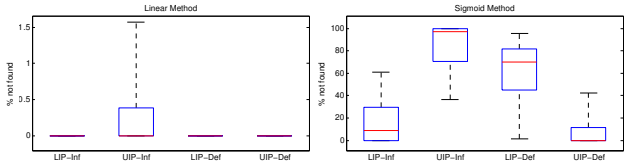

Fig. 2: How frequent each curve fitting method was able to locate an IP. The box around the median line represents the 75^{th} to 25^{th} quartile. The dashed lines outside of the box indicates the max and min values.

$$\text{Difference} = \text{Auto IP} - \text{Visual Heuristic IP} \tag{4}$$

In order to compare the linear and visual methods (4) was used and the median was found over the 5 participants then averaged over the 26 patients and over the 4 pixels. Similar inflection points were found between the linear and visual heuristic methods with the difference being -0.6247 mbar for the LIP and -0.4662 mbar for the UIP. Comparing the IP generated by the linear spline method and the visual heuristic method provides some insight to the accuracy of the linear based results since prior to function based curve fitting inflection points were located by eye [20], [21]. Fig. 3 shows the difference between the human inflection points and linear based inflection points.

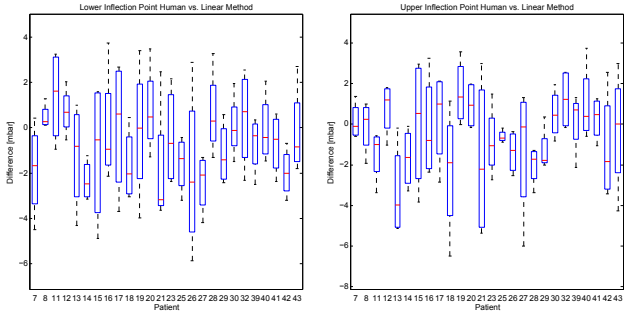

Fig. 3: Box plot showing the difference in IP from the human heuristics method and the linear spline method. The boxes around the median line represents the 75^{th} to 25^{th} quartile while the dashed lines represents the max and min for each difference.

C. Sigmoid vs. Visual Heuristic

Similar to the linear comparison (4) was used to compare the sigmoid method and visual heuristic method with the median being taken over the 5 participants then averaged over the 26 patients and 4 pixels. Larger differences were noticed with sigmoid method, compared to the linear vs. visual comparison. Differences of -2.09 mbar for the LIP and 2.6 mbar for the UIP were found. Additional to the larger differences the sigmoid method was again unable to find many IP. For this comparison a total of 147 of a possible 208 IP were not found, this is 70.7%. In Fig. 4 N/A represents no comparison was made due to a lack of IP found by the sigmoid method. Plots showing a single red line indicates only 1 of 4 IP were found by the sigmoid method.

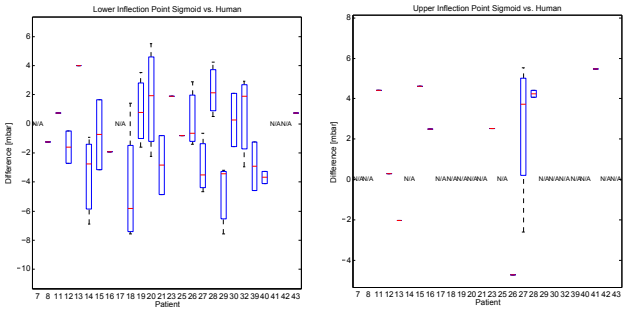

Fig. 4: Box plot showing the difference in IP from the human heuristics method and the linear spline method. The boxes around the median line represents the 75^{th} to 25^{th} quartile while the dashed lines represents the max and min for each difference. A lack of comparative data is represented by no quartile box surrounding the median. N/A means the sigmoid method was unable to find an inflection points for any of the four pixels.

IV. Discussion

Drawing conclusions from the comparisons it can be said that the linear method for locating inflection points from pressure-impedance graphs is worth using. The linear method allows for locating inflection points reliably. It is also easy to understand by doctors, providing easy to access standards. It also obtained similar results to the visual heuristic method showing its accuracy. Overall from the larger differences between the visual heuristic and sigmoid method as well as the lack of finding inflection points makes the linear spline method a better choice.

REFERENCES

[1] D. Schraufnagel, *Breathing in America: Diseases, Progress, and Hope*. American Thoracic Society, 2010.

[2] A. Hasan, *Understanding Mechanical Ventilation A Practical Handbook*. Springer-Verlab London Limited, 2010.

[3] M. H. Andersen, "Investigation of lung mechanics using CT scan analysis, a mathematical model and the static pressure volume curve," Master's thesis, Aalborg University, 2008.

[4] P. Neligan, "Pulmonary CCM tutorials," http://www.ccmtutorials.com/index.htm, 2006.

[5] R. S. Harris, D. R. Hess, and J. G. Venegas, "An objective analysis of the pressure-volume curve in the acute respiratory distress syndrome," *Am. J. Respir. Crit. Care Med.*, vol. 161, no. 2, pp. 432–439, 2000.

[6] J. G. Venegas, R. S. Harris, and B. A. Simon, "A comprehensive equation for the pulmonary pressure-volume curve," *Journal of Applied Physiology*, vol. 84, no. 1, pp. 389–395, 1998.

[7] D. Matamis, F. Lemaire, A. Harf, C. Brun-Buisson, J. C. Ansquer, and G. Atlan, "Total respiratory pressure-volume curves in the adult respiratory distress syndrome." *Chest*, vol. 86, no. 1, pp. 58–66, 1984.

[8] M. B. P. Amato, C. S. V. Barbas, D. M. Medeiros, R. B. Magaldi, G. P. Schettino, G. Lorenzi-Filho, R. A. Kairalla, D. Deheinzelin, C. Munoz, R. Oliveira, T. Y. Takagaki, and C. R. R. Carvalho, "Effect of a protective-ventilation strategy on mortality in the acute respiratory distress syndrome," *New England Journal of Medicine*, vol. 338, no. 6, pp. 347–354, 1998.

[9] A. J. S. Boyle, "The effect of shape deformation on two-dimensional electrical impedance tomography," Master's thesis, Carleton University, 2010.

[10] D. Holder, *Electrical Impedance Tomography: Methods, History, Applications*. Institute of Physics Publishing, 2004.

[11] L. Gattinoni, A. Pesenti, L. Avalli, F. Rossi, and M. Bombino, "Pressure-volume curve of total respiratory system in acute respiratory failure: Computed tomographic scan study," *Am. J. Respir. Crit. Care Med.*, vol. 136, no. 3, pp. 730–736, 1987.

[12] G. Hahn, I. Frerichs, M. Kleyer, and G. Hellige, "Local mechanics of the lung tissue determined by functional EIT," *Physiological Measurement*, vol. 17, no. 4A, p. A159, 1996.

[13] S. Pulletz, A. Adler, M. Kott, B. Elke, B. Hawelczyk, D. Schädler, G. Zick, N. Weiler, and I. Frerichs, "Regional lung opening and closing pressures in patients with acute lung injury," *Journal of Critical Care*, vol. 0000, no. 0000, p. 0000, 2011.

[14] B. Grychtol, G. K. Wolf, and J. H. Arnold, "Differences in regional pulmonary pressure impedance curves before and after lung injury assessed with a novel algorithm," *Physiological Measurement*, vol. 30, no. 6, p. S137, 2009.

[15] F. S. C. M. Rossi, R. S. Mascaretti, L. B. Haddad, N. A. Freddi, T. Mauad, and Rebello, "Utilization of the lower inflection point of the pressure-volume curve results in protective conventional ventilation comparable to high frequency oscillatory ventilation in an animal model of acute respiratory distress syndrome," *Clinics*, vol. 63, pp. 237–244, 00 2008.

[16] J. Hinz, O. Moerer, P. Neumann, T. Dudykevych, I. Frerichs, G. Hellige, and M. Quintel, "Regional pulmonary pressure volume curves in mechanically ventilated patients with acute respiratory failure measured by electrical impedance tomography," *Acta Anaesthesiologica*, vol. 50, no. 3, pp. 331–339, 2006.

[17] G. M. Albaiceta, F. Taboada, D. Parra, L. H. Luyando, J. Calvo, R. Menendez, and J. Otero, "Tomographic study of the inflection points of the pressure-volume curve in acute lung injury," *Am. J. Respir. Crit. Care Med.*, vol. 170, no. 10, pp. 1066–1072, 2004.

[18] J. D'Errico, "MATLAB central - file exchange," http://www.mathworks.com/matlabcentral/fileexchange/authors/679, 2011.

[19] R. S. Harris, "Pressure-volume curves of the respiratory system," *Respiratory Care*, vol. 50, no. 1, pp. 78–99, 2005.

[20] D. Matamis, F. Lemaire, A. Harf, C. Brun-Buisson, J. C. Ansquer, and G. Atlan, "Total respiratory pressure-volume curves in the adult respiratory distress syndrome." *Chest*, vol. 86, no. 1, pp. 58–66, 1984.

[21] L. Martin-Lefevre, J.-D. Ricard, E. Roupie, D. Dreyfuss, and G. Saumon, "Significance of the changes in the respiratory system pressure-volume curve during acute lung injury in rats," *Am. J. Respir. Crit. Care Med.*, vol. 164, no. 4, pp. 627–632, 2001.

[22] Merriam-Webster, "Medline plus - trusted health information for you," http://www.nlm.nih.gov/medlineplus/mplusdictionary.html, Jul. 2010.

[23] G. Bernard, A. Artigas, K. Brigham, J. Carlet, K. Falke, L. Hudson, M. Lamy, J. Legall, A. Morris, and R. Spragg, "The american-european consensus conference on ARDS. definitions, mechanisms, relevant outcomes, and clinical trial coordination," *Am. J. Respir. Crit. Care Med.*, vol. 149, no. 3, pp. 818–824, 1994.